POSTPRINT VERSION. The final version is published here :
Bencharif, L., Ouameur, M. A. et Massicotte, D. (2021, 13-15 Oct. 2021). Long Short-Term Memory for Indoor Localization Using WI-FI Received Signal Strength and Channel State Information. Communication présentée 2021 IEEE 4th 5G World Forum (5GWF), Montreal, Canada. doi: 10.1109/5GWF52925.2021.00047

Long Short-Term Memory for Indoor Localization Using WI-FI Received Signal Strength and Channel State Information

Lotfi Bencharif, Messaoud Ahmed Ouameur, and Daniel Massicotte

Université du Québec à Trois-Rivières, Department of electrical and computer engineering
Laboratoire des signaux et systèmes intégrés
{lotfi.bencharif, messaoud.ahmed.ouameur, daniel.massicotte}@uqtr.ca

Abstract— **Indoor location information is increasing in importance in contemporary communication services and applications. In this paper, we discuss the long short-term memory (LSTM) performance for indoor localization in non-line-of-sight (NLoS) conditions using the received signal strength (RSS) and channel state information (CSI) obtained from Wi-Fi signals. As such, we describe the CSI and RSS acquisition system that is used to build a rich dataset to experiment with classical machine learning and deep learning models. The distance range error matrix is combined with the confusion matrix to obtain the distance range error probability where we have demonstrated that the LSTM model exhibits a maximum range error of less than 5 m with 4% probability.**

Index Terms— Indoor localization, Deep learning (DL), Wi-Fi, Receiver signal strength (RSS), Channel state information (CSI), Long short-term memory (LSTM), Error probability.

I. Introduction

Presently, indoor localization is making the news in the high-tech and new technology sector. Indoor localization has recently received a lot of attention due to the potential use of a wide range of intelligent services. The exploitation of the Wi-Fi signal for calculating the location of a target device is one of the most widespread and sought-after technologies. In particular, Wi-Fi access points are widely deployed in any indoor environment. By analyzing different technologies and algorithms, we have concluded that the Wi-Fi-based method has proven to be a promising approach for determining the location of a device where existing indoor tracking methods rely on obtaining the channel state information (CSI), or obtaining approximate received signal strength (RSS) via a personal computer [1].

Indoor localization and navigation for mobile devices is a growing market with the expected size of 4 billion $ [1]. Indoor location information is growing in importance in modern communication services and applications [2] such as ambient assisted living and health applications for older adults by making them able to control their health conditions [3, 4]. Robotics is also one of the main applications of indoor localization to avoid obstacles [5]. Location is not only necessary for location-based services, it also has multiple uses in cyber-physical systems, such as intelligent transport systems and robotics in 5G networks [6].

Actually, these systems use radio signals, electromagnetic fields, or other information collected by different types of sensors with diverse technologies such as Wi-Fi, Bluetooth, ZigBee, and ultrasounds, to name a few [7]. These approaches vary significantly in terms of accuracy, coverage, efficiency, security, and reliability, which remain imperative obstacle in the indoor localization [7], [8]. Different indoor localization methods can be generally classified into three main groups according to the modelling information that are used: received signal strength (RSS)-based methods, angle-of-arrival (AoA)-based methods and time-of-arrival (ToA)-based localization algorithms [8] and channel state information (CSI).

For example, [8] and [2] discuss a customized UWB system and a modified Wi-Fi system to acquire metrics other than RSS. After transforming the 802.11 wideband signal into narrowband pulses, the WiSee system [9] uses Short Term Fourier Transform Pre-Processing (STFT) to derive different discriminating characteristics. Alternately, [2] presents an approach to indoor localization using a convolutional neural network (CNN) for channel classification and telemetry error regression on raw one-dimensional CSI traces. In [10], the authors present a deep learning (DL) approach using measures of transmission channel quality, including RSS and channel state information (CSI). They divide a rectangular room plan into two-dimensional blocks. Each block is treated as a class and defines the location as a classification problem. Using RSS and CSI, they developed four deep neural networks implemented using multi-layer perceptrons (MLPs) and one-dimensional convolutional neural networks (1-D-CNN) to estimate the position of objects in the room. Experimental results show that the 1-D-CNN network using CSI information can achieve excellent positioning performance. In [8] the authors used the long short-term memory (LSTM) for activity recognition in addition to other conventional machine learning (ML) techniques, such as the hidden Markov model (HMM). Even if the LSTM approach suffers from long training time, it is shown to outperform the ML techniques.

The traditional fingerprint-based Wi-Fi positioning system is easy to measure and requires little hardware, so RSS vectors from different access points are used as fingerprints. However, even in a static environment, the instability of RSS will change over time at a fixed location. Furthermore, RSS is approximate information, which can lead to confusion between adjacent locations and ultimately reduce the performance of the positioning system. With the development of a new generation of Wi-Fi Network Interface Cards (NICs) supporting IEEE 802.11n, with Orthogonal Frequency Division Multiplexing (OFDM) and Multiple Input Multiple Output (MIMO) technologies, it is now possible to extract the channel state information (CSI) from certain NICs, such as Intel Wi-Fi Wireless Link 5300.

The main contributions of this paper are:

1. We describe our WIFI CSI acquisition system that we used to acquire both the RSS and the CSI.
2. We exploit the RSS and the CSI using machine and deep learning techniques for indoor localization applications. Particularly, we will introduce the LSTM model in comparison with other techniques such as those studies in [2], [8] and [10]. To our knowledge, *this is the first work that uses both RSS and CSI with LSTM model*. The proposed model outperforms state of the art proposals in [2] and [8] while competing those proposals that use deep convolutional neural networks such as [10].
3. Finally, since the localization problem is treated as a classification problem, a localization error range is presented to *evaluate the models beyond the coarse localization accuracy performance metric* where the minimum and maximum distance range matrix is combined with the confusion matrix to obtain the distance range error probability.

The paper is organized as follows: Section II describes the system architecture while Section III discusses the measurements and the dataset. In Section IV, the LSTM model is presented and optimized to address the indoor localization application as a classification problem. Therein, the localization error range analysis is discussed. Finally, the conclusions are drawn and some future research directions are outlined in Section V.

II. System Architecture

The system architecture for indoor localization is conceptually depicted in Fig. 1. The CSI is measured at the physical layer to obtain reliable communication. With firmware modification, the CSI is accessible via the upper layer. A CSI acquisition tool based on the Intel Wi-Fi 5300 Network Interface Card [7] is used to measure CSI. The *receiver* uses the Intel NIC 5300 to receive data from the transmitter, namely the TP-Link gateway.

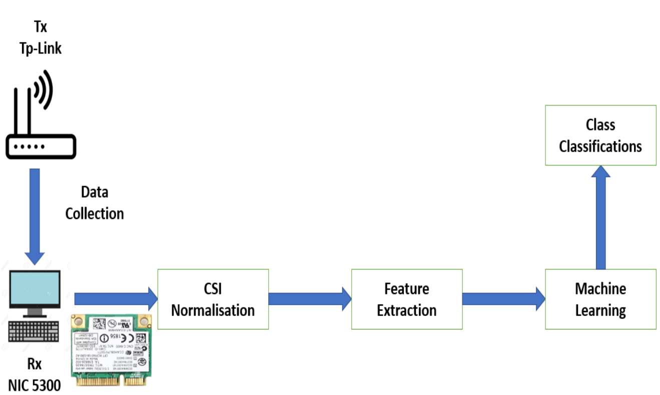

Fig. 1 System architecture for indoor localization with Intel NIC5300 as a receiver and TP-Link as a transmitter.

On the other hand, a personal computer (PC) runs a Matlab-based script to retrieve the collected data. The same PC leverage the machine and deep learning models and tools to implement the indoor localization application as a classification task.

III. Measurements and Dataset

This section outlines the measurement procedures for collecting the indoor non-line-of-sight (NLoS) classification dataset. The measurement campaign includes the collection of a NLoS dataset at the campus of the université du Quebec à Trois-Rivières (UQTR, Quebec, Canada). The placement of access points (APs) and laptops is fixed and known a priori (see Fig. 2.a). By changing the place of the transmitter in a lab, the receiver can record different raw CSI and RSS and form a training dataset.

Localization performance is generally affected by the complexity of the indoor environment. In order to evaluate the robustness of the proposed method, we chose the *signal and integrated system's laboratory* at UQTR (see Fig.2.a) while

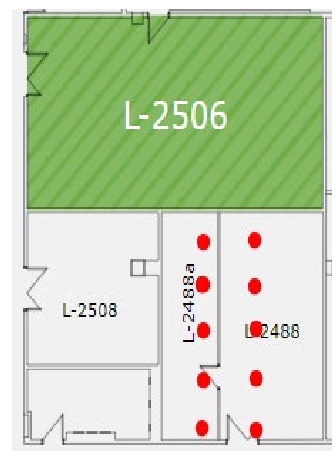

a)

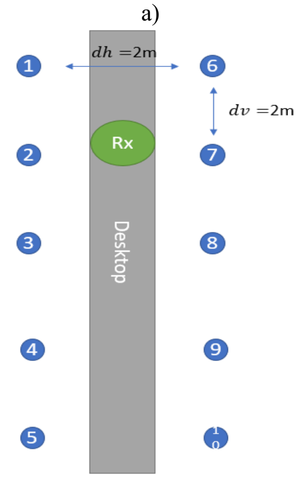

b)

Fig. 2 a) Experimental environment location at UQTR, and b) the measurement reference points at the signal and integrated system's laboratory at UQTR (2488LP) where horizontal distance is $d_h = 2$m and the vertical distance is $d_v = 2$m

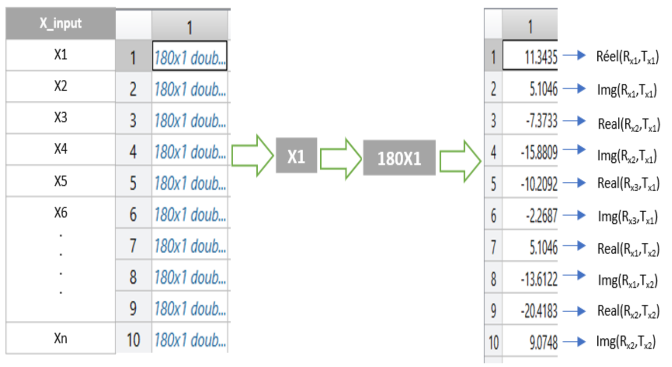

Fig. 3 Data preprocessing for each measurement point

adding a reasonable number of obstacles (regular chairs and tables we find in a typical lab/office) to increase the complexity of the environment.

The lab is an enclosed space of 8.37 metres long and 7.44 metres wide. The rectangular area between the offices in the room is divided into 10 points. The centre of each point is the reference point (or training point), as indicated by the blue circle in Fig. 2.b. It is worth noting that similar experimentations were conducted in a residential house and other facilities. However, due to lack of space and similar findings we focus on the lab location at UQTR.

As depicted in Fig. 1, to build a ML classification model for indoor localization, an extensive dataset representing 10 distinct locations is needed. Since it is very time consuming to build an extensive dataset with a large number of predefined node locations, we have limited our experimentation to 10 distinct points to demonstrate how to leverage the RSS and the CSI. The transmitter (gateway) is positioned in a fixed location based on the 10 points as shown in Fig. 2.b.

n = 7500 measurements in total were made at every point, with almost equal data sizes between locations. The collected dataset is organized in the X_input cell array that contains cells X1 to Xn, each cell contains is 180 ×1 measurement vector. A given vector contains the real and the imaginary parts (2x) of the complex valued CSI of the 30 subcarriers of a system operating in 1x3 MIMO mode. Note that figure 3 shows a 2x3 MIMO mode, however, most location were acquired with only a single transmit antenna. Let's take an example of the first cell (see Fig. 3): the first entry represents the real value of the CSI at the first receive antenna from the first transmit antenna, the second entry represents the imaginary value of the CSI at the first receive antenna from the first transmit antenna, entry 9 represents the real value of the CSI at the second receive antenna from the second transmit antenna, while entry 10 represents the imaginary value of the CSI at the second receive antenna from the second transmit antenna as depicted in Fig. 3.

IV. Indoor Localization

This section addresses the LSTM model-based classification. LSTM is an artificial recurrent neural network (RNN) architecture. An LSTM unit is commonly composed of a cell, an input gate, an output gate and a forget gate [11]. The cell recalls values at arbitrary time intervals while the three gates regulate the flow of information into and out of the cell. In other words, the previous network state is not wasted and the previous state is utilized for the next prediction.

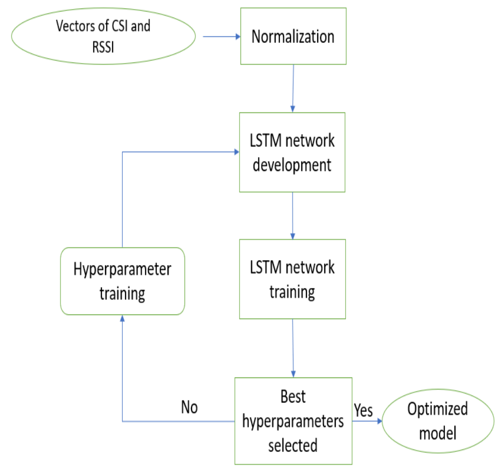

Fig. 4 Flowcharts of the hyperparameter selection process

Table 1. Optimal LSTM parameters

Optimizer	Adam
Learning Rate	0.0065
Input Layer	180
Number of Hidden Layers	400
Batch Size	2000
Max Epoch	50
L2Regularization	0.001

As shown in Fig. 4, 180 ×1 vectors of CSI and RSS values are provided to the system as input. The input data is first normalized using max-min normalization. A portion (70%) of the input CSI and RSS vectors are used to train the LSTM model. A grid search of the model hyperparameters is performed. By examining the training and validation curves, we deduced the optimal value of the hyperparameters. Table 1 depicts the optimal values of these hyperparameters [chap. 6 of 11].

A. Measurements of RSS and CSI

Figures 5 and 6 show the RSS and the absolute CSI over 30 subcarriers in dB scale, respectively. The different colors in the figures indicate the signals measured at different locations/measurement point. The measurements were shown for two different points to illustrate that the changes produced by RSS are relatively small, meaning that RSS is less sensitive to environmental changes than CSI.

B. LSTM model's evaluation

In order to evaluate our proposed model (Table 1), the dataset is divided into two categories: training and validation. We collected a total of 6 000 training samples and 1 500 validation samples.

On the other hand, we have experimented with several ML models which are implemented using Matlab® Toolbox. These models include Weighted KNN (W-KNN), quadratic support vector machines (Q-SVM), fine KNN and kernel naïve bayes (KNB). Only the variants with the highest accuracy are shown in Table 2. One can clearly see that both the LSTM and Q-SVM are demonstrating outstanding accuracies at 99% and 98%,

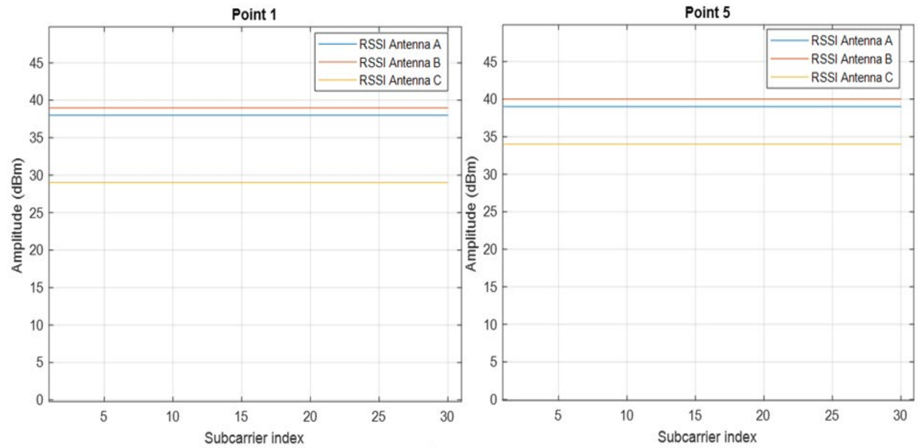

Fig. 5 RSS waveforms measured at different reference points.

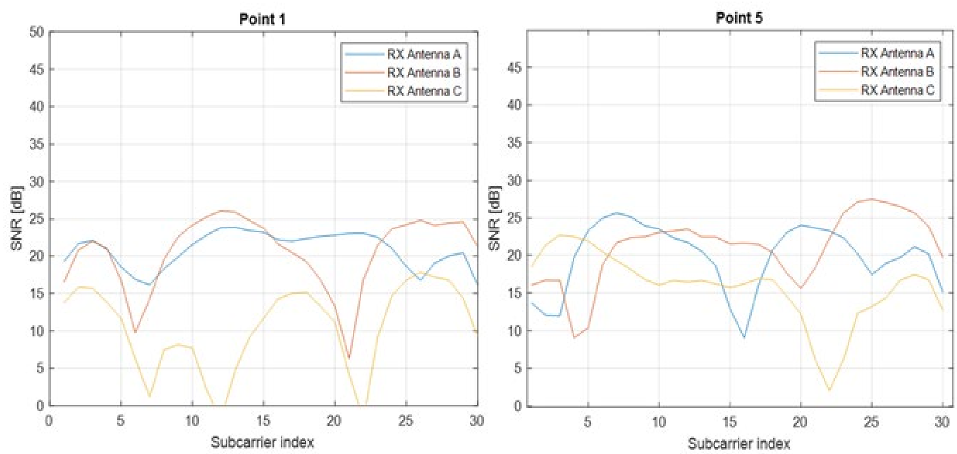

Fig. 6 CSI waveforms measured at different reference points.

respectively, if both the RSS and CSI at different receiving antennas are well exploited (not shown here for the lack of space, the accuracy is 96% and 97% without RSS). This outperformes state of the art proposals in [2] and [8] while competing those proposals that use deep convolutional neural networks such as [10]. Unfortunately, such coarse accuracy metric does not tell the whole story about the localization error. For instance, one would be interested to know what is the classification error rate for a given range in meters.

C. *Localization error analysis*

This paper presents localization as a classification problem and uses the prediction accuracy or prediction error rate to evaluate localization performance.

As we discussed earlier, we divide our lab into 2-by-5 blocks. If the target is in a block (class) and what is predicted in another block (class), the location system will issue a classification error and the location error is proportional to the distance between the target block and the predicted one. In this subsection, our goal is to convert the prediction error rate to the location error, which meets the requirements for the location task. The location error is the distance between the position of the reference point and the estimated position [10].

Table 2. Comparison of prediction accuracy (%)

Reference points	LSTM	Q-SVM	W-KNN	Fine KNN	KNB
1	94.7	95.7	90.5	92.5	86.4
2	100.0	96.9	97.3	98.3	100
3	100.0	98.8	95.1	98.4	100
4	100.0	99.9	99.6	99.9	99.9
5	100.0	99.5	96.7	97.9	99.9
6	96.7	99.1	72.5	84.1	91.5
7	100.0	97.3	90.1	88.1	96.9
8	100.0	100.0	98.8	98.0	100
9	100.0	98.0	93.7	97.1	84.3
10	98.7	98.7	93.2	92.8	99.5
Average	**99.00**	**98.40**	**92.81**	**94.71**	**95.84**

(a) Localization error for correct prediction

In the case of correct prediction, the predicted block is the target block. In this case, we will consider point 1 as a reference point, the minimum localization error is $d_{min} = 0$ and the maximum locates error $d_{max} = \sqrt{(0.5d_h)^2 + (0.5d_v)^2}$ where horizontal distance is $d_h = 2$m and the vertical distance is $d_v = 2$m.

Table 4. Comparison of localization error probability (%) of various methods for the reference point # 1 (in Fig. 2)

Error Range (m)	LSTM	Q-SVM	W- KNN	Fine KNN	KNB
[0.00, 1.41]	94.7	95.7	90.5	92.5	86.4
[1.00, 3.16]	0	0	0	0	0
[1.00, 3.16]	0	0	0	0.1	0
[1.41, 4.24]	4.6	0.9	0.8	0.1	12.9
[3.00, 5.10]	0	0	0.1	0	0
[4.24, 5.83]	0	0.7	1.1	1.6	0
[5.00, 7.07]	0.7	2.7	2.9	2.7	0.7
[5.83, 7.62]	0	0	0	0	0
[7.00, 9.06]	0	0	0	0	0
[7.62, 9.49]	0	0	4.5	2.9	0

(b) Localization error for incorrect prediction

In the case of incorrect prediction, the prediction is not the target. There are three situations in this case:

- Horizontal error

Suppose the reference point is in the center of block i, then the estimated position will be at any position of the other block j in the horizontal direction. In addition, the maximum localization error exists when the estimate is in the top right or bottom right corner of block j. We can calculate the minimum and maximum error as

$$d_{min} = d_h(|j-i| - 0.5) \tag{1}$$

$$d_{max} = \sqrt{((|j-i| + 0.5)d_h)^2 + (0.5d_v)^2} \tag{2}$$

where $i, j = 1,2, \ldots, 5$, d_h is the distance between two horizontal neighbours and d_v is the distance between two vertical neighbours. In our implementation $d_h = 2m$ and $d_v = 2m$.

- Vertical error

It is assumed that the reference point is in the middle of the block i and that the estimated location at any position of the other block j will be in the vertical direction.

$$d_{min} = d_h(|j-i| - 4.5) \tag{3}$$

$$d_{max} = \sqrt{((|j-i| - 4.5)d_h)^2 + (|j-i| - 3.5)d_v)^2} \tag{4}$$

- Oblique error

Table 5. Comparison of location accuracies (%) for different measurement methods based on RSS and CSI.

Methods	Accuracy (%)
SVM [2]	82.50
MLP [2]	82.90
CNN [2]	87.40
LSTM [8]	90.50
HMM [8]	73.30
Random forest [8]	64.60
CNN [10]	99.98
MLP [10]	99.93
Proposed LSTM	99.00
Proposed Q-SVM	98.40

In this case, the estimated position at each position of the other block j will be in the oblique direction of the reference point. we can calculate the minimal and maximal error as

$$d_{min} = \sqrt{((|j-i| - 5 - 0.5)d_h)^2 + (0.5d_v)^2} \tag{5}$$

$$d_{max} = \sqrt{((|j-i| - 5 + 0.5)d_h)^2 + (1.5d_v)^2} \tag{6}$$

As depicted in Table 3, using the formulas (1) to (6) we obtain a 10-by-10 matrix of distance $[d_{ij}]$ where each entry has two values, a minimum localization error d_{min} and a maximum localization error d_{max}.

Combining the distance range error matrix with the confusion matrix, we obtain the distance range error probability $p(d)$, as shown in Table 4 for the reference point # 1 (in Fig. 2).

Based on the worst accuracy performance using point # 1, the LSTM model shows the smallest error probability for distance range errors above 5 m.

It shall be noted that the literature in this field is very promising for obtaining good precision in indoor environments. However, there are still challenges for future work, such as how to use CSI phase information in addition to amplitude, how to stabilize the system in different dynamic environments, and how to calculate localization error for correct prediction. Nevertheless, for the sake of completeness, Table 5 represents the performance of proposed LSTM in comparison with other approaches as reported in references [2], [8] and [10]. It is time consuming to rigorously implement the models in [2], [8] and [10]. It is also out of the scope of the current work to provide

Table 3. 10-by-10 distance range error matrix $[d_{min}, d_{max}]$ (referred to Fig. 2 for 10-point location)

	1	2	3	4	5	6	7	8	9	10
1	[0.00, 1.41]	[1.00, 3.16]	[3.00, 5.10]	[5.00, 7.07]	[7.00, 9.06]	[1.00, 3.16]	[1.41, 4.24]	[4.24, 5.83]	[5.83, 7.62]	[7.62, 9.49]
2	[1.00, 3.16]	[0.00, 1.41]	[1.00, 3.16]	[3.00, 5.10]	[5.00, 7.07]	[7.00, 9.06]	[1.00, 3.16]	[1.41, 4.24]	[4.24, 5.83]	[5.83, 7.62]
3	[3.00, 5.10]	[1.00, 3.16]	[0.00, 1.41]	[1.00, 3.16]	[3.00, 5.10]	[5.00, 7.07]	[7.00, 9.06]	[1.00, 3.16]	[1.41, 4.24]	[4.24, 5.83]
4	[5.00, 7.07]	[3.00, 5.10]	[1.00, 3.16]	[0.00, 1.41]	[1.00, 3.16]	[3.00, 5.10]	[5.00, 7.07]	[7.00, 9.06]	[1.00, 3.16]	[1.41, 4.24]
5	[7.00, 9.06]	[5.00, 7.07]	[3.00, 5.10]	[1.00, 3.16]	[0.00, 1.41]	[1.00, 3.16]	[3.00, 5.10]	[5.00, 7.07]	[7.00, 9.06]	[1.00, 3.16]
6	[1.00, 3.16]	[7.00, 9.06]	[5.00, 7.07]	[3.00, 5.10]	[1.00, 3.16]	[0.00, 1.41]	[1.00, 3.16]	[3.00, 5.10]	[5.00, 7.07]	[7.00, 9.06]
7	[1.41, 4.24]	[1.00, 3.16]	[7.00, 9.06]	[5.00, 7.07]	[3.00, 5.10]	[1.00, 3.16]	[0.00, 1.41]	[1.00, 3.16]	[3.00, 5.10]	[5.00, 7.07]
8	[4.24, 5.83]	[1.41, 4.24]	[1.00, 3.16]	[7.00, 9.06]	[5.00, 7.07]	[3.00, 5.10]	[1.00, 3.16]	[0.00, 1.41]	[1.00, 3.16]	[3.00, 5.10]
9	[5.83, 7.62]	[4.24, 5.83]	[1.41, 4.24]	[1.00, 3.16]	[7.00, 9.06]	[5.00, 7.07]	[3.00, 5.10]	[1.00, 3.16]	[0.00, 1.41]	[1.00, 3.16]
10	[7.62, 9.49]	[5.83, 7.62]	[4.24, 5.83]	[1.41, 4.24]	[1.00, 3.16]	[7.00, 9.06]	[5.00, 7.07]	[3.00, 5.10]	[1.00, 3.16]	[0.00, 1.41]

in-depth discussion and comparison against other localization systems that resorts to UWB, Bluetooth and ZigBee signals.

V. Conclusion

In this paper, we have presented an indoor Wi-Fi based localization system, which can acquire RSS and CSI information. A 99% classification accuracy can be easily obtained using DL models such as LSTM and even a simple quadratic support vector machines (Q-SVM) can reach more than 98% accuracy if both CSI and RSS information are well exploited. The proposed model outperforms state of the art proposals in [2] and [8] while competing those proposals that use deep convolutional neural networks such as [10]. Unfortunately, such aggregate score does not tell the whole story. As such combining the distance range error and the confusion matrix one can readily predict the distance range error probability.

Acknowledgements

This work has been funded by the Natural Sciences and Engineering Research Council of Canada grant and the Canada Foundation for Innovation, the CMC Microsystems.

References

[1] M. Ahmed Ouameur, M. Caza-Szoka, and D. Massicotte, "Machine learning enabled tools and methods for indoor localization using low power wireless network," Internet of Things, Volume 12, 2020.

[2] K. Bregar and M. Mohorčič, "Improving indoor localization using convolutional neural networks on computationally restricted devices," IEEE Access, vol. 6, pp. 17429-17441, 2018.

[3] D. U. Khan, K. A. Siek, J. Meyers, L. M. Haverhals, S. Cali, and S. E. Ross, "Designing a personal health application for older adults to manage medications," in Proceedings of the 1st ACM International Health Informatics Symposium, pp. 849-858, 2010.

[4] I. Qudah, P. Leijdekkers, and V. Gay, "Using mobile phones to improve medication compliance and awareness for cardiac patients," in Proceedings of the 3rd International Conference on PErvasive Technologies Related to Assistive Environments, pp. 1-7, 2010.

[5] S. Mastellone, D. M. Stipanović, C. R. Graunke, K. A. Intlekofer, and M. W. Spong, "Formation control and collision avoidance for multi-agent non-holonomic systems: Theory and experiments," The International Journal of Robotics Research, vol. 27, no. 1, pp. 107-126, 2008.

[6] R. C. Daniels and R. W. Heath, "Link adaptation with position/motion information in vehicle-to-vehicle networks," IEEE transactions on wireless communications, vol. 11, no. 2, pp. 505-509, 2011.

[7] V. Bianchi, P. Ciampolini, and I. De Munari, "RSSI-based indoor localization and identification for ZigBee wireless sensor networks in smart homes," IEEE Transactions on Instrumentation and Measurement, vol. 68, no. 2, pp. 566-575, 2018.

[8] S. Yousefi, H. Narui, S. Dayal, S. Ermon, and S. Valaee, "A survey on behaviour recognition using wifi channel state information," IEEE Communications Magazine, vol. 55, no. 10, pp. 98-104, 2017.

[9] T. Taleb and A. Kunz, "Machine type communications in 3GPP networks: potential, challenges, and solutions," IEEE Communications Magazine, vol. 50, no. 3, pp. 178-184, 2012.

[10] C.-H. Hsieh, J.-Y. Chen, and B.-H. Nien, "Deep Learning-Based Indoor Localization Using Received Signal Strength and Channel State Information," IEEE Access, vol. 7, pp. 33256-33267, 2019.

[11] S. Raschka , V. Mirjalili , Python Machine Learning, 3rd Ed, Packt Publishing, 2019.